X-ray Fluorescence Analysis of Hexavalent Chromium Using Kβ Satellite Peak Observed as Counterpart of X-ray Absorption Near-Edge Structure Pre-Edge Peak

ARTICLE *in* ANALYTICAL CHEMISTRY · AUGUST 2011

Impact Factor: 5.64 · DOI: 10.1021/ac201606c · Source: PubMed

2 AUTHORS, INCLUDING:

Isao Tsuyumoto
Kanazawa Institute of Technology
54 PUBLICATIONS **483** CITATIONS

SEE PROFILE

analytical chemistry

TECHNICAL NOTE

pubs.acs.org/ac

X-ray Fluorescence Analysis of Hexavalent Chromium Using Kβ Satellite Peak Observed as Counterpart of X-ray Absorption Near-Edge Structure Pre-Edge Peak

Isao Tsuyumoto* and Yoshihiro Maruyama

Department of Applied Chemistry, College of Bioscience and Chemistry, Kanazawa Institute of Technology, 7-1 Ohgigaoka, Nonoichi, Ishikawa 921-8501, Japan

ABSTRACT: A Kβ satellite peak in X-ray fluorescence (XRF) spectra is observed as a counterpart of the pre-edge peak of the X-ray absorption near edge structure (XANES). In Kβ emission of chromium, a small satellite peak is observed at 5.983−5.988 keV only for hexavalent chromium compounds such as CrO_3, $Na_2CrO_7 \cdot 2H_2O$, $Na_2CrO_4 \cdot 4H_2O$, $K_2Cr_2O_7$, K_2CrO_4, $Zn_2CrO_4(OH)_2 \cdot 2H_2O$, $PbCrO_4$, and $BaCrO_4$, together with the main peak at 5.947 keV, while trivalent chromium compounds such as Cr_2O_3 and $Cr(OH)_3 \cdot nH_2O$ show only the main peak at 5.947 keV. This corresponds to the fact that the K pre-edge peak in XANES is observed only for the hexavalent chromium compounds. The electronic level causing the satellite peak is almost at the same energy level as that causing the pre-edge peak. Our finding not only affects the interpretation of the origin of the pre-edge peaks but also leads to the simple speciation method of chromium compounds using XRF.

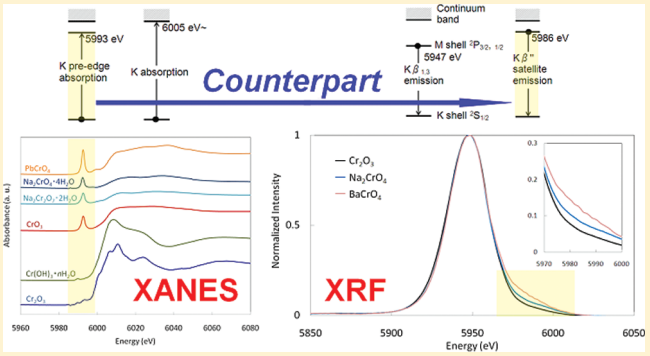

An understanding of valence states of heavy metals in the environment is essential to assess potential hazards because the toxicity of the heavy metals varies greatly and is dependent on the chemical states.[1] It is well-known that there is a great difference in toxicity between hexavalent and trivalent chromium compounds, and in many countries only the hexavalent chromium is strictly regulated. Since the hexavalent chromium compounds have higher solubilities in water than the trivalent chromium compounds, discrimination between them have been generally made by combination of elution tests and element analyses in the area of environmental analysis. Analysis of trace amounts of hexavalent chromium (~6.4 mass ppm of Cr(VI) in 58.4 mass ppm of total Cr) has been also achieved by using X-ray absorption near-edge structure (XANES) spectroscopy.[2,3] Because hexavalant chromium exhibits a distinct Cr K pre-edge peak about 12 eV prior to the main Cr K absorption edge as shown in Figure 1, the intensity of the Cr K pre-edge peak has been used for quantitative analysis of the hexavalent chromium. This pre-edge absorption resonance has been considered to be due to electronic transitions from 1s to 3d and sometimes characteristic to transition metals with empty d orbitals. These pre-edge features are also observed for Ti(IV), V(V), Mn(VII), and etc. and have been extensively investigated by many researchers.[4−13] Although the transition from 1s to 3d is a dipole forbidden transition, it can gain intensity by a quadrupole transition from 1s to 3d or a dipole transition from 1s to a d−p hybrid orbital. Numerous precise measurements and theoretical calculations have been performed to estimate the

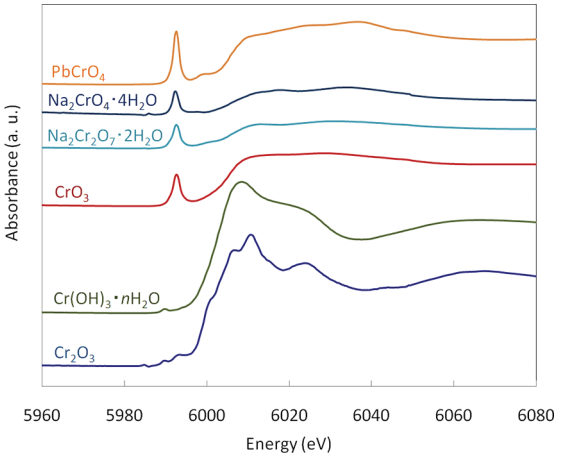

Figure 1. XANES K-edge spectra for Cr_2O_3, $Cr(OH)_3 \cdot nH_2O$, CrO_3, $Na_2Cr_2O_7 \cdot 2H_2O$, $Na_2CrO_4 \cdot 4H_2O$, and $PbCrO_4$. The spectra are vertically deviated for clarity.

contributions of such mechanisms to the pre-edge peaks, and it has been deduced that the electric quadrupole transition from 1s to 3d is an erroneous interpretation.[14] The pre-edge is related to the coordination structure of the central transition metal ion, and

Received: June 23, 2011
Accepted: August 26, 2011
Published: August 26, 2011

it can be interpreted through the O_h and T_d character tables of group theory. The same discussion is also applicable to Kβ X-ray fluorescence spectra.[15,16]

Many researchers have intensively investigated the fine structures of X-ray fluorescence (XRF) spectra.[17−20] It has been reported that the oscillation similar to the extended X-ray absorption fine structure (EXAFS) was observed in lower energy than the main Kα peak of XRF and that the similar information as EXAFS spectra was obtained without using a synchrotron radiation facility.[21−25] Fluorescence spectra generally show counterparts of absorption spectra because both involve transitions among the same electronic levels. There have, however, been no reports on the fine structures of the XRF spectra showing the counterpart of the XANES pre-edge peak. In this study, we present the first observation of the counterpart of the pre-edge peak of Cr K-edge absorption spectra in Cr Kβ emission spectra.

EXPERIMENTAL SECTION

Two types of trivalent chromium compounds and eight types of hexavalent chromium compounds were measured: Cr_2O_3, $Cr(OH)_3\cdot nH_2O$, CrO_3, $K_2Cr_2O_7$, K_2CrO_4, $Na_2Cr_2O_7\cdot 2H_2O$, $Na_2CrO_4\cdot 4H_2O$, $Zn_2CrO_4(OH)_2\cdot 2H_2O$, $PbCrO_4$, and $BaCrO_4$ (Kanto Chemical Co., Inc., Tokyo, Japan; reagent grade). Each sample was pressed into a pellet of 13 mm o.d. In order to examine the relationship between the Cr(VI)/total Cr ratio and the satellite peak intensity, five types of a mixed pellet of Cr_2O_3 and $Na_2CrO_4\cdot 4H_2O$ were also measured. As for $Cr(OH)_3\cdot nH_2O$, BN was mixed with $Cr(OH)_3\cdot nH_2O$ to improve the stiffness of the pellet at the ratio of 1 part BN to 4 parts $Cr(OH)_3\cdot nH_2O$ by weight.

XRF spectra were taken with a wavelength dispersive X-ray fluorescence spectrometer (XRF-1700; Shimadzu Co., Ltd., Kyoto, Japan). A rhodium anode X-ray tube was used for excitation with 40 kV and 95 mA. The dispersive crystal was LiF (200) ($2d$ = 0.40267 nm), and the X-ray detector was a scintillation counter with NaI (Tl). The 2θ scan range was from 57° to 65° by a 0.01°step, and the counts were accumulated for 50 s for each step. The XRF spectra were fitted with a pseudo-Voigt function and a Lorentz function using a nonlinear least-squares method based on the generalized reduced gradient algorithm. XANES spectra, for comparison, were also taken for Cr_2O_3, $Cr(OH)_3\cdot nH_2O$, CrO_3, $Na_2Cr_2O_7\cdot 2H_2O$, $Na_2CrO_4\cdot 4H_2O$, and $PbCrO_4$ at beamline BL38B01 of Spring-8 (Japan Synchrotron Radiation Research Institute, JASRI; Hyogo, Japan).[3] The spectra were collected in transmission mode using two ion chambers for I_0 and I.

RESULTS AND DISCUSSION

In the XANES spectra, a single peak was observed in the pre-edge region of the spectra of the hexavalent chromium compounds, at about 12 eV smaller than the Cr K absorption edge, and the pre-edge peak was not observed for the trivalent chromium compounds, as shown in Figure 1. Figure 2 shows Cr Kβ XRF spectra after background subtraction and normalization. All the spectra were almost the same around the main peak K$\beta_{1,3}$ ($^2P_{3/2}$, $^2P_{1/2} \rightarrow {}^2S_{1/2}$) at 5.947 keV. However, a small shoulder was observed only for hexavalent chromium compounds in the tail region of 5.97−6.00 keV. The spectral curves for CrO_3, $K_2Cr_2O_7$, K_2CrO_4, $Na_2Cr_2O_7\cdot 2H_2O$, $Na_2CrO_4\cdot 4H_2O$, $Zn_2CrO_4(OH)_2\cdot 2H_2O$, and $PbCrO_4$ were almost the same, whereas the curve for $BaCrO_4$ showed a larger shoulder than the other hexavalent compounds. Similarly the spectral curves for Cr_2O_3 and $Cr(OH)_3\cdot nH_2O$ were almost the same. The main peak was well fitted with the pseudo-Voigt function, except for the small shoulder region of hexavalent chromium compounds. The residual error after subtracting the fitted pseudo-Voigt function from the experimental data indicated that a small satellite peak (we call this here Kβ'') existed around 5.99 keV in the spectra of the hexavalent chromium compounds. Thus, the double-peak fitting, the pseudo-Voigt function for the main peak and the Lorentzian function for the satellite peak, was performed. The residual sum of squares for the hexavalent chromium compounds were substantially reduced by using the double-peak fitting, whereas those for the trivalent chromium compounds remained almost the same as the case of the single peak fitting. The fitting parameters are summarized in Table 1. The satellite peak of hexavalent chromium compounds except for $BaCrO_4$ is centered at 5.986−5.988 keV, about 40 eV higher than the main peak at 5.947 eV, and the intensity is about 4% of the main peak. As for $BaCrO_4$, the satellite peak is centered at 5.983 keV, and the intensity is about 7% of the main peak. Figure 3 shows the relationship between the Cr(VI)/total Cr ratio and the satellite peak area. The satellite peak was estimated to show small intensity also for the sample with no hexavalent chromium because of the small deviation between the experimental data of the main peak and the fitted pseudo-Voigt function. Such phenomena are usually

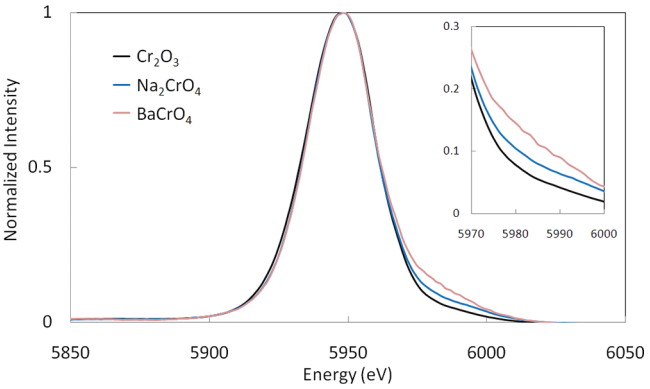

Figure 2. Kβ emission spectra for Cr_2O_3, Na_2CrO_4, and $BaCrO_4$. The inset is a magnified image of satellite regions.

Table 1. Peak Parameters of Kβ Emissions for Chromium Compounds[a]

	main peak				satellite peak		
	u (eV)	σ (eV)	h	η	u (eV)	σ (eV)	h
CrO_3	5947	13	1.026	0.355	5986	9	0.036
Na_2CrO_4	5947	13	1.078	0.459	5986	10	0.043
$Na_2Cr_2O_7$	5947	13	1.044	0.355	5986	10	0.040
K_2CrO_4	5948	13	1.053	0.354	5987	11	0.045
$K_2Cr_2O_7$	5947	13	1.036	0.342	5986	10	0.043
$ZnCrO_4$	5948	13	1.040	0.382	5987	10	0.041
$PbCrO_4$	5947	13	1.060	0.383	5988	12	0.042
$BaCrO_4$	5947	13	1.030	0.454	5983	11	0.069
Cr_2O_3	5947	13	1.057	0.327			
$Cr(OH)_3$	5947	13	1.056	0.366			

[a] u, peak position; σ, FWHM; h, peak height; and η, ratio of Lorentz function in pseudo-Voigt function.

dx.doi.org/10.1021/ac201606c |Anal. Chem. 2011, 83, 7566–7569

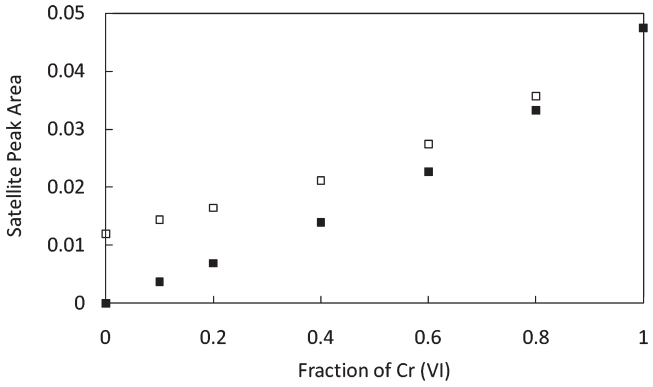

Figure 3. The satellite peak area vs hexavalent chromium content for five mixtures of Cr_2O_3 and Na_2CrO_4. The satellite peak area is normalized to the main peak area. The open square, □, shows the observed peak area (I_{obs}) containing the contribution from the trivalent chromium, which is derived from the deviation between the main peak and the fitted function. The closed square, ■, shows the net peak area (I_{net}) calculated by canceling the apparent contribution of the trivalent chromium.

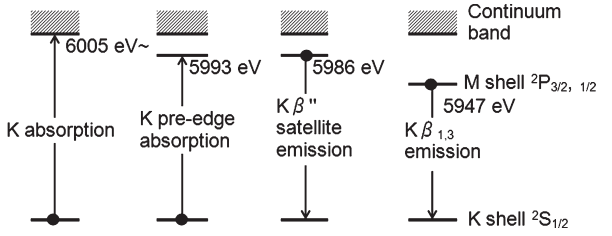

Figure 4. Schematic illustration of the origin of the Kβ'' satellite emission and the K-pre-edge absorption along with the ordinary K$\beta_{1,3}$ emission and K-edge absorption.

observed in the multiparameter fitting process. In order to cancel the apparent contribution of the trivalent chromium derived from the deviation between the theoretical and experimental curves, the net satellite peak area (I_{net}) was estimated by subtracting the satellite peak area at the fraction of Cr(VI) = 0 from the observed peak area (I_{obs}),

$$I_{net} = I_{obs} - (1 - f_{hex})I_0 \quad (1)$$

where f_{hex} is the fraction of Cr(VI) and I_0 is the observed satellite peak area at f_{hex} = 0. The calibration curve for the fraction of Cr(VI) vs the net satellite peak area showed a linear relationship. This indicates that the quantitative analysis of valence states will be possible by the analysis of the satellite peak in the XRF spectra.

Figure 4 shows the comparison between the energy levels of K absorption and Kβ emission. The energy level to which an electron transits in the K pre-edge absorption (5.993 keV) is very close to the energy level from which an electron transits in the present Kβ'' satellite emission (5.983−5.988 keV). Therefore, the satellite peak observed only for the hexavalent chromium compounds is a counterpart of the pre-edge peak of XANES observed only for the same hexavalent chromium compounds as well. This is the first observation of the counterpart of the pre-edge peak of XANES in the XRF spectra. The origin of the pre-edge peak in XANES has been considered to be due to the electric quadrupole transition from 1s to 3d or the electric dipole transition from 1s to a d−p hybrid orbital. Recent studies based on polarized spectra, group theory, and theoretical calculations indicated that an intense pre-edge peak is attributable to the electric dipole transition to p-character in the d−p hybrid orbital and that the electric quadrupole transition from 1s to 3d is the erroneous interpretation.[14]

The pre-edge features are characteristic to the transition metals with empty 3d orbital such as Cr(VI), Ti(IV), V(V), and Mn(VII). It is interesting to note that not only the transition to the electronic level corresponding to the pre-edge feature in XANES but also the transition from the same electronic level was observed in XRF. Because the 3d orbital is empty, the quadrupole transition from 3d to 1s in XRF is considered to be improbable. Our results also contradict the quadrupole transition and support the electric dipole transition from the d−p hybrid orbital relating to the symmetry of the central transition metal ion. We expect the analysis of the satellite peaks in XRF spectra would be very informative to clarify the origin of the pre-edge features, because they contain useful information on the electronic levels relating to the XANES.

The main peaks observed in the present study were rather broad (fwhm, 0.33°, 0.013 keV), and the satellite peaks were superimposed on the tail of the main peaks. The energy resolution would be greatly improved by employing a double crystal X-ray monochromator or the Bragg-Brentano geometry,[26] and simple and easy analysis without using the synchrotron radiation facility would be possible. The pre-edge peaks in XANES reflect various information on the chemical states of metal compounds such as symmetry, valence, and coordination number.[11] The analysis of the fine structure of XRF spectra would be an effective tool alternative to the conventional XANES analysis to obtain such information. We believe that our present findings in the fine structure of XRF spectra would promote the field of chemical state analysis.

■ CONCLUSIONS

We first found that the fine structures of Kβ emission in XRF spectra provide the same information as the K pre-edge feature of XANES spectra. In Kβ emission, a small satellite peak at 5.983−5.988 keV was observed only for hexavalent chromium compounds, about 40 eV higher than the main peak at 5.947 keV, corresponding to the fact that K pre-edge peaks are observed at 5.993 keV only for hexavalent chromium compounds in XANES spectra. As for the origin of the pre-edge peaks and the corresponding satellite peaks, our results contradict the quadrupole transition and support the electric dipole transition from the d−p hybrid orbital. Since the pre-edge peaks in XANES reflect the chemical states of metal compounds such as symmetry, valence, and coordination number, it is expected that the analysis of the fine structures of XRF would be a new useful tool for chemical state analysis.

■ AUTHOR INFORMATION

Corresponding Author

*E-mail: tsuyu@neptune.kanazawa-it.ac.jp.

■ REFERENCES

(1) Hesterberg, D.; Sayers, D. E.; Zhou, W.; Plummer, G. M.; Robarge, W. P. *Environ. Sci. Technol.* **1997**, *32*, 2840–2846.

(2) Tsuyumoto, I.; Uchikawa, H. *J. Am. Ceram. Soc.* **2004**, *87* (12), 2294–2296.

(3) Tsuyumoto, I.; Uchikawa, H. *J. Ceram. Soc. Jpn.* **2003**, *111* (8), 608–610.

(4) Yamamoto, T.; Mizoguchi, T.; Tanaka, I. *Phys. Rev. B* **2005**, *71*, 245113.
(5) Mizoguchi, T.; Tanaka, I.; Yoshioka, S.; Kunisu, M.; Yamamoto, T.; Ching, W. Y. *Phys. Rev. B* **2004**, *70*, 045103.
(6) George, S. D.; Brant, P.; Solomon, E. I. *J. Am. Chem. Soc.* **2005**, *127*, 667–674.
(7) Wu, Z. Y.; Xian, D. C.; Hu, T. D.; Xie, Y. N.; Tao, Y.; Natoli, C. R.; Paris, E.; Marcelli, A. *Phys. Rev. B* **2004**, *70*, 033104.
(8) Pantelouris, A.; Modrow, H.; Pantelouris, M.; Hormes, J.; Reinen, D. *Chem. Phys.* **2004**, *300*, 13–22.
(9) Shaffer, R. E.; Cross, J. O.; Rose-Pehrsson, S. L.; Elam, W. T. *Anal. Chim. Acta* **2001**, *442*, 295–304.
(10) Groot, F. *Chem. Rev.* **2001**, *101*, 1779–1808.
(11) Westre, T. E.; Kennepohl, P.; DeWitt, J. G.; Hedman, B.; Hodgson, K. O.; Solomon, E. I. *J. Am. Chem. Soc.* **1997**, *119*, 6297–6314.
(12) Lee, J. F.; Bajt, S.; Clark, S. B.; Lamble, G. M.; Langton, C. A.; Oji, L. *Physica B* **1995**, *208/209*, 577–578.
(13) Bajt, S.; Clark, S. B.; Sutton, S. R.; Rivers, M. L.; Smith, J. V. *Anal. Chem.* **1993**, *65*, 1800–1803.
(14) Yamamoto, T. *X-Ray Spectrom.* **2008**, *37*, 572–584.
(15) Torok, I.; Papp, T.; Palinkas, J.; Budnar, M.; Muhleisen, A.; Kawai, J.; Campbell, J. L. *Nucl. Instrum. Methods Phys. Res., Sect. B* **1996**, *114*, 9–14.
(16) Kawai, J.; Nakamura, E.; Nihei, Y. *Spectrochim. Acta* **1990**, *45B*, 463–479.
(17) Bergmann, U.; Glatzel, P.; Degroot, F.; Cramer, S. P. *J. Am. Chem. Soc.* **1999**, *121*, 4926–4927.
(18) Holzer, G.; Fritsch, M.; Deutsch, M.; Hartwig, J.; Forster, E. *Phys. Rev. A* **1997**, *56*, 4554.
(19) Kawai, J.; Maeda, K.; Nakajima, K.; Gohshi, Y. *Phys. Rev. B* **1993**, *48*, 8560.
(20) Kawai, J.; Takami, M.; Satoko, C. *Phys. Rev. Lett.* **1990**, *65*, 2193.
(21) Szaloki, I.; Torok, S. B.; Ro, C.; Injuk, J.; Grieken, R. V. *Anal. Chem.* **2000**, *72*, 211R–233R.
(22) Kawai, J.; Hayashi, K.; Tanuma, S. *Analyst* **1998**, *123*, 617–619.
(23) Kawai, J.; Hayachi, K.; Okuda, K.; Nisawa, A. *Chem. Lett.* **1998**, 245–246.
(24) Hayashi, K.; Kawai, J.; Awakura, Y. *Spectrochim. Acta* **1997**, *B52*, 2169–2172.
(25) Tohji, K.; Udagawa, Y. *Phys. Rev. B* **1989**, *39*, 7590.
(26) Hayakawa, S.; Gohshi, Y.; Iida, A.; Aoki, S.; Sato, K. *Rev. Sci. Instrum.* **1991**, *62*, 2545–2549.